SSRG International Journal of Electronics and Communication Engineering
ISSN: 2348-8549/ https://doi.org/10.14445/23488549/IJECE-V11I7P108

Volume 11 Issue 7, 77-88, July 2024

Original Article

Path Loss Performance Analysis of Low Power IEEE 802.11af Secondary TV White Space Devices Based on Field Measurements

Alberto S. Banacia[1], Rosana J. Ferolin[2]

[1]*Department of Electrical and Electronics Engineering, University of San Carlos, Cebu City, Philippines.*
[2]*School of Engineering, University of San Carlos, Cebu City, Philippines.*

[1]*Corresponding Author : asbanacia@usc.edu.ph*

Received: 06 May 2024 Revised: 06 June 2024 Accepted: 05 July 2024 Published: 27 July 2024

Abstract - *The IEEE 802.11af standard is a wireless local area network that operates in the television white space, requiring it to avoid inducing damaging interference to licensed users such as incumbent digital and television services. To achieve this, precise tools for estimating path loss are essential to prevent both underestimation and overestimation, which could either limit the coverage of White Space Devices (WSDs) or fail to adequately shield primary or licensed users from unwanted emissions produced by secondary WSDs. This paper examines and compares the performance of various models for path loss, including Free Space Path Loss (FSPL), relevant portions of Recommendation ITU-R P.1411-11, and the linear and logarithmic regression models, against field measurement data to identify the most suitable path loss estimation model. The findings indicate that the logarithmic regression model exhibits the Root-Mean-Square Error (RMSE) that has the best performance, with a mean estimation error of 5 dB across all experimental locations where measurements were conducted. Additionally, the study suggests that the path loss model for free space can effectively provide a conservative path loss estimate for all sites, with an average overestimation of 18 dB, thereby ensuring adequate protection for primary users against potential interference from secondary users.*

Keywords - *IEEE 802.11af, Path loss, TV white space.*

1. Introduction

Since its inception, the TV white space tests and deployment initiatives have gained momentum worldwide with varying applications like linking a far-flung community in Bhutan (Asia Pacific) to quality health care to streaming daily live recordings in a London zoo of animals on YouTube (Europe); to providing broadband connectivity to select schools within a 10 – kilometre radius in Cape Town, South Africa (Africa) interference-free to primary users of licensed spectrum. The technology has proven its ability to address the gap in the digital divide and accessibility to inexpensive internet connectivity especially in distant areas hardly or yet to be reached by broadband services [1].

The Institute of Electrical and Electronics Engineers (IEEE) developed and issued in 2013 the IEEE 802.11af standard as a Wireless Local Area Network (WLAN) that is based on cognitive radio technology and operates in TV white space [2]. It permits unlicensed or primary users to opportunistically and dynamically use the unoccupied frequency in the TV band. In [3], the IEEE 802.22 as a backhaul and the IEEE 802.11af device were interfaced to demonstrate the possibility of extended internet coverage using these white space devices. The same devices were used both as Access Points (APs) and Stations (STAs) to implement a multi-hop network [4] successfully. This demonstrated the ability of this standard to create an Information and Communications Technology (ICT) network that is robust and easily deployable, especially in times of calamities. Further, in a suburban environment, devices compliant with IEEE 802.11af standard successfully demonstrated Vehicle to Infrastructure communications (V2I) and Vehicle to Vehicle (V2V) communications [5, 6].

But just like any other TV white space devices, the operation of devices that follow the IEEE 802.11af specifications should ensure the protection of Primary Licensed Users (PUs) such as incumbent Digital TV (DTV) broadcast services at all times by not causing harmful interference to it. Figure 1 shows the basic concept of TV white space regulation and operation. A primary user, such as a TV broadcast station assigned to operate at channel k, has a predefined service contour that serves as a protected area of operation for the station. A TV white space secondary users

must not be permitted to operate inside this protected service contour until the 4 km to 31.2 km additional separation keeps out the distance that must be tracked from the edge of the safe-guarded area [7]. To be able to comply with this requirement, an accurate model to predict path loss must be utilized to prevent overestimation that unnecessarily limits the regions where white space devices can operate or underestimate path loss that results in insufficient protection of primary users from destructive interference originating from WSDs. An IEEE 802.11af–compliant device must use path loss models that are essential in defining appropriate locations for access points that will ensure optimum coverage area. It also aids in assessing the hazards of interference that IEEE 802.11af - compliant devices may cause to licensed existing users.

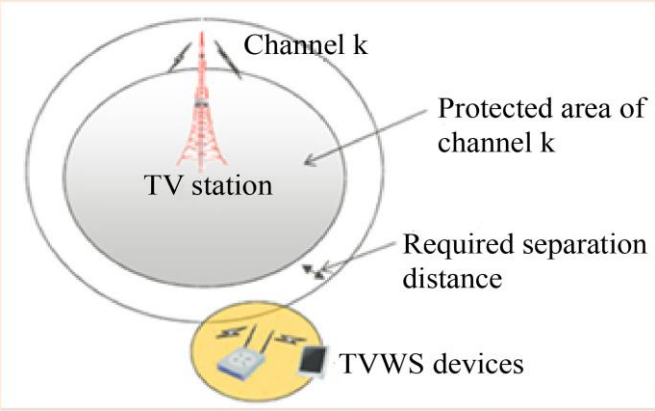

Fig. 1 TVWS device regulation basic concept [7]

This study, conducted within the University premises, involved measuring propagation loss in a low-rise urban/suburban setting. The aim was to assess the effectiveness of various models for path loss, including Free Space Path Loss (FSPL), pertinent sections of ITU-R P.1411-11 Recommendation, as well as linear and logarithmic regression models that were compared on the basis of field measurement data to define the model that can give the most accurate estimation of path loss. The findings revealed that the logarithmic regression model exhibited the Root-Mean-Square Error (RMSE) that has the best performance, with a mean estimation error of 5 dB across all three test locations in the measurement campaign. Additionally, the study concludes that the path loss model for free space can reliably provide a conservative estimate for all sites, with an average overestimation of 18 dB, thereby ensuring adequate protection for primary users against potential interference risks from secondary TV white space devices.

This paper is organized as follows: Section 2 discusses the literature review, and Section 3 details the experimental locations and measurement setup, with accompanying illustrations. This is followed by Section 4, which outlines the path loss models and associated calculations. Section 5 examines and evaluates the results, while Section 6 concludes the study.

2. Literature Review

Path loss, also known as attenuation, refers to the decrease in strength of a radio frequency signal as it propagates from the transmitting source to the receiving destination through a communication channel, leading to diminished received signal power. This phenomenon is typically quantified in Decibels (dB). Several factors contribute to path loss, including transmitter power, gains of the antenna, frequency, and the transmitter-receiver distance [9]. Path loss prediction models serve as essential tools in the design and optimization of performance for most networks and applications.

In reference [9], the parameters for the path loss model for both Line-of-Sight (LoS) and Non-Line-of-Sight (NLoS) environments were derived through an indoor experiment conducted as part of the pilot program of the United Kingdom's Office of Communications (Ofcom). This study also analyzed the measured path loss variation in indoor propagation utilizing IEEE 802.11af prototype devices and using log-normal and extreme value statistical distributions. Further, the same study examined the characterization and throughput estimation of the devices' performance. In reference [10], the potential interference-free coexistence among DTV receivers and IEEE 802.11af transmitters was investigated by determining the mandatory separation distance between the protected channel area and the TVWS device through the application of ITU-R P.1411-7 recommendations. The latter specifies guidance on calculation techniques and data propagation for designing short-range outdoor radio communication systems and local networks within 0.3 to 100 GHz. Previous studies cited in references [12-15] utilized the same recommendation to compute the networks' path loss. Specifically, references [14, 15] applied it to predict path attenuation for planning 802.11n networks operating in urban areas.

In an agricultural area, to estimate large scale fading at 433 MHz of transmitted radio signals along various routes, measurement campaigns were performed to acquire topographical profile and path loss data. Using the measured data, the models were then fitted [16]. Path loss estimation models based on the principle of and procedure in Machine-learning were presented in [17]. On the other hand, [18] made use of environmental feature extraction of images taken from satellites to improve path loss prediction. A recent study used Artificial Intelligence techniques to model path loss for networks in diverse settings for cellular mobile [19].

Some studies used regression models to study and measure path loss or signal attenuation. Linear regression over networks with communication guarantees was studied in [20] while presented in [21] as an Access Point that served as a basis for indoor localization and used regression to investigate and quantify the amount of signal reduction triggered by the complex interior surroundings. Linear regression was also applied for Wireless Sensor Network time synchronization

[22]. To optimize a wireless sensor network for a smart city application, a study conducted in [23] presented a model that is based on linear regression.

Based on the works mentioned above, it can be deduced, except for the study in [4], that not much attention has been given to path loss prediction models for low-power IEEE 802.11af-based networks deployed outdoors. Considering that this network operates on a spectrum-sharing principle hence, interference with primary users must be avoided, and this matter must be addressed. This paper summarizes and evaluates the performance of some path loss models, including Free Space (FSPL), ITU-R P.1411-11 Recommendation, linear and logarithmic regression models, and compared them against the data obtained from field measurement to obtain the prediction model that best suits a network that conforms with the IEEE 802.11af standard and prototypes.

3. Experimental Sites, NICT Devices and Measurement Setup

3.1. Experimental Site

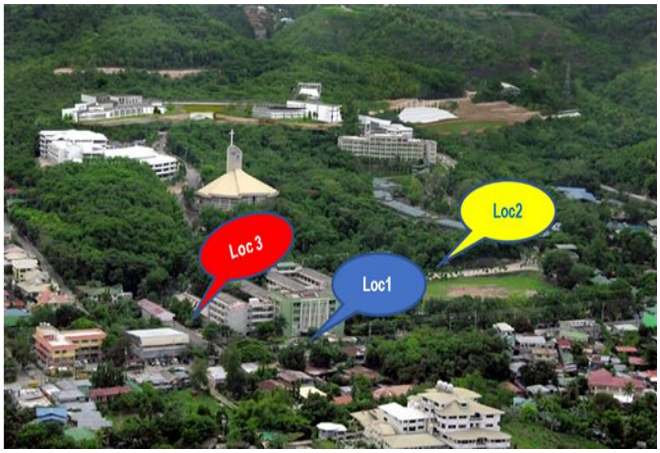

Fig. 2 Aerial view of USC-Talamban Campus

Figure 2 shows the aerial view of the University premises where the radio field tests were performed, and measurements were obtained. It is a private Catholic university located in Cebu City, Philippines that measures a land area of approximately 83 hectares. Only a limited number of buildings can be found inside its premises, while the remaining area is open vegetation. The building structures inside are mostly made of concrete bodies or frames, wooden doors and window glasses. These buildings have a height that normally runs from 15 m to 20 m. The hilly landscape makes it an appropriate representation of mountains and foliage in the middle of the AP and STA of a wireless network.

The three selected experimental sites within the campus were chosen to reflect different suburban transmission environments. Location 1 (Loc1) is a dual street with a lane that measures 15 meters in width, bordered by a pedestrian road lined with residential houses and low-rise structures. On the left side are rows of trees extending approximately 100 meters alongside a 5-story building. This location spans around 170 meters from the University's main gate to the first gate, although only about 150 meters were included in the research due to either dead zones or weak, intermittent signals within the first 20 meters. Location 2 (Loc2) features a 10-meter road nestled amidst a row of trees, with minimal vehicular and pedestrian traffic. It extends for a total of 155 meters. Lastly, Location 3 (Loc3) consists of a 20-meter road flanked by low-rise edifices on either side, surpassing the antenna height of both the AP and STA. This location spans approximately 290 meters. Across all sites examined in this study, there exists a direct Line-of-Sight (LoS) between the Access Point (AP) and Station (STA).

3.2. NICT Prototype Devices and Measurement Setup

The radio equipment utilized in this research, serving both as a transmitter and receiver, is the prototype manufactured by Japan's National Institute of Information and Communications Technology (NICT), the IEEE 802.11af. This device conforms to the guidelines set by the European Telecommunication Standards Institute.

The Physical (PHY) and Medium Access Control (MAC) parameters of the prototype are outlined in [2]. It features a maximum 20 dBm power output and possesses 30 x 23 x 20 cubic cm dimensions. Figure 3 depicts both the front and rear views of the device. The available Modulation and Coding Scheme (MCS) ranges from index 0 to index 7, with achievable data rates for a single spatial stream detailed in [24]. However, for this study, only MCS0 is employed, utilizing BPSK modulation with a coding rate of ½.

Figure 4 illustrates the measurement setup used throughout the conduct of this study. A 1.7 m-high AP was used as the transmitter with 20 dBm transmit power. The STA, with a height of 1.2 m, was configured similarly to that of the AP. An omnidirectional whip antenna with an isotropic gain of about 2.2 dB was used for both devices. An SMA-SMA RF cable was used to connect the antenna to the NICT device. The cable is assumed to have a cable loss of 1.0 dB. Throughout the measurement campaign, the channel bandwidth was set at 6 MHz, centred at 593 MHz. This is equivalent to the Philippines' UHF Channel 34. At each experimental location, the position of the Access Point was fixed while the Station was moved every 5 meters from the AP. At each position, the received signal power was measured in dBm, averaged in a 2-minute duration, and then recorded.

Based on the mentioned parameters, measurements were taken and then fitted to the free space model, to the appropriate sections of ITU-R P.1411 – 11 Recommendations, and the linear and logarithmic regression models to determine the path loss prediction method that best fits the gathered and recorded data.

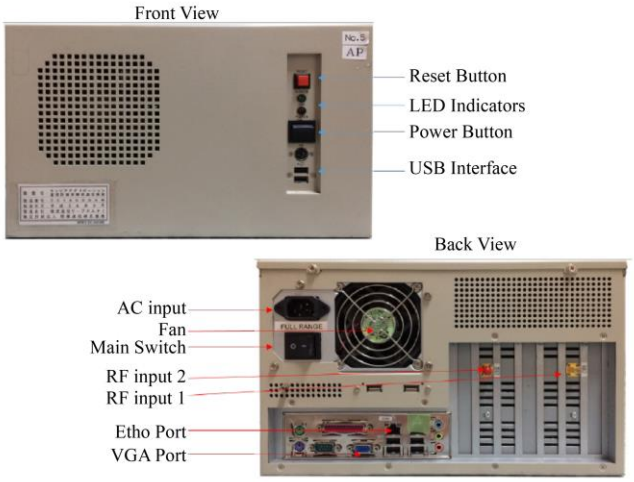

Fig. 3 Front and rear view of the IEEE 802.11af Prototype built by NICT

Fig. 4 Measurement setup illustration

4. Path Loss Models and RMSE Computations

The IEEE 802.11af standard operates on the principle of cognitive radio. As a WLAN function within a TV band, the utilization of path loss models becomes crucial. These models serve as essential tools for determining optimal locations for Access Points, thereby ensuring the widest possible signal coverage. By accurately predicting path loss, network planners can strategically deploy Access Points to maximize coverage while minimizing interference and signal degradation, thus enhancing the overall reliability and performance of the network. As a secondary device, it must also prevent destructive interference to prevailing licensed, primary users such as DTVs. Hence, precise path loss estimation models for white space devices become indispensable to avoid overestimation that will needlessly limit the regions where the white space devices can function or to prevent path loss underestimation that will fail to shield DTVs from damaging interference coming from WSDs. The following models for path loss were considered in this study:

4.1. Measured Path Loss (MPL) Computation

The measured strength of signal power is converted to measured path loss by means of Equation 1.

$$\text{Measured Path Loss (dB)} = \mathrm{Pt_{dBm}} + \mathrm{Gt_{dB}} + \mathrm{Gr_{dB}} + \mathrm{Pr_{dBm}} \quad (1)$$

Where, $\mathrm{Pt_{dBm}}$ is the 20 dBm AP transmitter power fixed for all field experiments conducted in this study, $\mathrm{Pr_{dBm}}$ is the recorded signal power at the receiving STA, $\mathrm{Gt_{dB}}$ and $\mathrm{Gr_{dB}}$ are the AP and STA antenna gain, respectively, which were both fixed at 2.2 dB isotropic.

4.2. Path Loss Model in Free Space

Free Space Path Loss (FSPL) is a popular prediction model for estimating the amount of signal power received when there is a clear, unhindered, direct path separating the transmitter from the receiver. Similar to many radio wave propagation models that are large-scale, the FSPL model estimates that received signal strength deteriorates in accordance with the Tx - Rx separation distance raised to some power. In free space, Friis's formula expresses the antenna received power originating from a transmitting antenna at a distance d as

$$\mathrm{Pr(d)} = \frac{\mathrm{PtGtGr}\lambda^2}{(4\pi)^2\mathrm{d}^2\mathrm{L}} \quad (2)$$

$P(d)$ depends on various factors: Pt denotes the transmitted power, Gt and Gr represent respectively the transmit and receive antenna gains. d stands for the Tx – Rx separation, while λ represents the wavelength. Both d and λ are expressed in meters. Additionally, system loss not associated with propagation is denoted by L.

The variance between the transmitted power and the received power is what constitutes path loss. Measured and expressed in Decibels (dB) as a positive quantity representing signal attenuation, it may or may not include antenna gains, but when excluded, the antenna gain is assumed to be of unity value. Equations 3 and 4 define two mathematical expressions for the free space path loss model as

$$\mathrm{FSPL} = 10\log\frac{\mathrm{Pt}}{\mathrm{Pr}} = -10\log\left(\frac{\lambda^2}{(4\pi)^2\mathrm{d}^2}\right) \quad (3)$$

$$\mathrm{FSPL} = 32.45 + 20\log\mathrm{f_{MHz}} + 20\log\mathrm{d_{Km}} \quad \mathrm{dB} \quad (4)$$

The received power Pr obtained from the Friis free space equation is valid only if obtained for distances d that are within the propagating antenna's far field region [8].

4.3. ITU-R P.1411 – 11 Recommendation [11]

The Recommendation is applied in the range spanning 0.3 to 100 GHz, specifically for short-range outdoor propagation scenarios. It guides fundamental transmission loss models

tailored for NLoS and LoS conditions, as well as multipath models suitable for environments like street canyons and areas with over rooftops. Additionally, it addresses factors such as building entry loss, the count of signal components, fading effects, and polarization characteristics. Compatibility studies can also utilize this Recommendation. For this work, only Sections 4.1.2 and 4.3.1 were considered.

4.3.1. Section 4.1.2 Line-of-Sight (LoS) path

Three levels of station location are considered in ITU – R P.1411. Nevertheless, this study focuses on a specific scenario where the Access Point is positioned beneath the rooftop but overhead level, while the Station is situated at head level. This setup mirrors a micro- or pico-cellular network communication setting, typically found in low-rise urban or suburban areas, where signal transmission primarily occurs within street canyons. Consequently, the site-specific model outlined in Section 4.1.2 was utilized accordingly.

With the two-ray plane model as the basis, Equation 5 defines the approximate lower bound (LoS_L) for signal transmission in the UHF range as follows.

$$L_O S_L = L_{bp} + \begin{cases} 20\log_{10}\left(\frac{d}{Rbp}\right) & \text{for } d \le Rbp \\ 40\log_{10}\left(\frac{d}{Rbp}\right) & \text{for } d > Rbp \end{cases} \quad (5)$$

The breakpoint distance R_{bp} in meters is estimated using the formula

$$R_{bp} \approx \frac{4HtxHrx}{\lambda} \quad (6)$$

Here, Hrx and Htx represent the receiving and transmitting antenna height, respectively, and λ denotes the wavelength. All measurements are in meters. Equation 7 provides an approximate upper limit for Line-of-sight (LoS_U) concerning distances shorter than, equal to, or greater than R_{bp} expressed as

$$L_O S_U = L_{bp} + 20 + \begin{cases} 25\log_{10}\left(\frac{d}{Rbp}\right) & \text{for } d \le Rbp \\ 40\log_{10}\left(\frac{d}{Rbp}\right) & \text{for } d > Rbp \end{cases} \quad (7)$$

At the breakpoint, *Lbp* represents the fundamental propagation loss calculated as:

$$L_{bp} = 20\log_{10}\left(\frac{\lambda^2}{8\pi HtxHrx}\right) \quad (8)$$

The 20 dB in Equation 7 is the upper bound fading margin.

4.3.2. Section 4.3.1 Site-General Model

Section 4.3.1 presents the model designed for signal transmission between AP and STA terminals, positioned from beneath rooftop height to proximate street level. This model encompasses statistical data on location variability for LoS and NLoS areas. The model is derived from studies performed with antenna heights ranging from 1.9 to 3.0 meters above ground level, AP – STA separation extending up to 3 kilometers, and is applicable within the frequency of 0.3 to 3 GHz. The necessary parameters for this model include the frequency f in Megahertz and the separation distance d in meters between the devices. This research work only includes those with LoS links with the variability of location at a distance d (LoS(d,p)) defined in Equation 9 as:

$$LoS(d,p) = 32.45 + 20log_{10}f + 20log_{10}\left(\frac{d}{100}\right) + \Delta LoS(p) \quad (9)$$

Given the location percentage p(%) and δ = 7 dB, the ΔLoS(p) is given as:

$$\Delta\text{LoS(p)} = 1.5624\Delta\left(\left(\sqrt{-2\ln\left(1-\frac{p}{100}\right)}\right) - 1.774\right) \quad (10)$$

4.4. Regression Models [25], [26], [27]

A statistical technique for approximating the relationships between one or more independent variables (also referred to as 'predictors' or 'explanatory variables') and a dependent variable (frequently termed the 'response' or 'outcome' variable) is known as Regression analysis while a regression model specifies a function that describes the correlation between these variables. Regression analysis is primarily applied for prediction or, forecasting or inferring causal relationships between the dependent and independent variables. It generates a mathematical model to describe the statistical correlation between variables. In this section, regression analysis is applied as a modelling technique to find a curve (or line) that best models or fits the data collected from real-world observations. In this study, linear and logarithmic models were considered in predicting path loss in dB.

For both the linear and logarithmic regression models, the R^2 value or the determination coefficient is computed. R^2 measures statistically how the fitted regression line accurately represents the measured or observed data. While the lower value of Root Mean Squared Error (RMSE) implies a regression model with higher accuracy, however, a higher value of R – squared is deemed necessary. In the linear regression model, R-squared is used to indicate how effectively the independent variables account for the variability in the dependent variable. It is the ratio of the sum of squares of residuals from the regression model (SSE) and the Total Sum of Squares (SST) of errors from the average model subtracted from 1. Mathematically, it is defined as

$$R^2 = 1 - \frac{SSE}{SST} = 1 - \frac{\sum(y_i - \bar{y})^2}{\sum(y_i - \bar{y})^2} \quad (11)$$

R^2 ranges from 0 to 1, with values near 1 signifying a better fit of the regression model to the data.

4.4.1. Linear Regression

The most common form of regression analysis consisting only of one response or dependent variable y and one explanatory or independent variable x where the relationship between these variables is modeled using basic algebra is

simple linear regression. It does this by essentially fitting a best-fit line and observing how the data is spread around this line.

If the population parameters, β_0 and β_1, are known, the simple linear regression equation is written as :

$$E(y) = \beta_0 + \beta_1 x \quad (12)$$

Where, for a given value of x, $E(y)$ is the mean value of y; β_0 is the y - intercept population parameter, and β_1 is the slope population parameter. But in reality, population parameters are hardly available. Therefore, these parameters are estimated using sample data as follows:

$$\hat{y} = b_0 + b_1 x \quad (13)$$

Where, b_0 is the sample intercept that estimates the population intercept β_0; and b_1 is the sample slope that estimates the population slope β_1.

The following formulas are used to solve for b_0 and b_1, respectively:

$$b_0 = \bar{y} - b_1 \bar{x} \quad (14)$$

$$b_1 = \frac{\sum(x_i - \bar{x})(y_i - \bar{y})}{\sum(x_i - \bar{x})^2} \quad (15)$$

Where, $\bar{x}$ is the mean of the independent or explanatory variable; x_i is the i-th value of the independent variable; $\bar{y}$ is the mean of the dependent variable; y_i is the i-th value of the response variable (observed or measured value), and $\hat{y}_i$ is the estimated (predicted) value of the dependent variable.

4.4.2. Logarithmic Regression

Logarithmic regression is commonly employed to model real-world phenomena exhibiting rapid initial growth or decay followed by a gradual slowdown over time.

This regression type finds practical applications in various scenarios, such as measuring sound intensity, monitoring pH levels in solutions, predicting yields in chemical reactions, forecasting production levels of goods, and in numerous other contexts. When doing logarithmic regression analysis, the logarithmic function popularly used, and is used as well in this study, is defined as follows:

$$\hat{y}_i = b_0 + b_1 \ln x_i \quad (16)$$

Where, $\hat{y}_i$ is the estimated loss in dB; b_1 the coefficient that controls the rate of growth ($b_1 > 0$) or decay ($b_1 < 0$); $x_i$is the distance in meters and b_0 is the constant or y-intercept. Note that the line curve always passes through$(1, b_0)$. Note further that Equation 16 is a log transformation that involves the transformation of only the independent variable x_i. This suggests that a 1% increase in the independent variable x_i is linked to a linear change of $b_1/100$ or 0.01 x b_1 units in the dependent variable $\hat{y}_i$.

4.4.3. Root Mean Square Error (RMSE)

In statistical prediction models, predicted values seldom exactly match actual outcomes, producing a difference between them known as the residual (or error). In this work, RMSE is used as a tool for evaluating the prediction models' performance considered in this research work. It is the square root of the residuals or errors'variance that measures the deviation of the average error of recorded propagation loss to quantities estimated by the path loss model in free space, the appropriate sections of ITU – R P.1411, as well as values predicted by the linear and logarithmic regression models. If the primary purpose of the model is prediction, then RMSE is the most important criterion as it is a good indicator of how precise the model can predict the outcome. A better fitting model results from having a lower value of RMSE. To calculate RMSE, each error is squared and then averaged. Squaring ensures that errors in one direction do not offset errors in the other direction. Then, finally, the square root is computed. Mathematically, RMSE is calculated using Equation 17 below:

$$\text{RMSE} = \sqrt{\frac{\sum_{i=1}^{n}(y_i - \hat{y}_i)^2}{n}} \quad (17)$$

Where, y_i is the recorded/observed path loss for each location i, where measurements were taken; $\hat{y}_i$ is the propagation loss predicted per model per location i where measurements were taken.

5. Results and Discussion

5.1. Free Space Propagation Model (FSPL)

As expected, in this path loss model, attenuation in dB increases with increasing distance between the AP and STA, and this is true for all test locations considered in this study, as shown in Figure 5. In all sites where there exists a LoS environment, propagating signals are reduced over distance according to the square power law closely following Friis' free space path loss equation. Notice how in the same Figure 5 all the data points in each site were located above the orange line representing the FSPL graph. This means that FSPL underestimated path loss, resulting in RMSE values of 14.22 dB (Location 1), 20.72 dB (Location 2), and 18.73 dB (Location 3) as listed in Table 1.

In practical terms, an average underestimated path loss of 18 dB translates to causing undue interference coming from IEEE 802.11af devices to existing licensed primary users. In a standard that operates on the concept of cognitive spectrum sharing, this scenario must be avoided at all times, making the use of FSPL as a path loss model ill-suited to ensuring protection to primary users. However, the primary usage of FSPL for the IEEE 802.11af device, as shown in the location of the various measured path losses, is its ability to provide sufficient lower bounds in all sites, which in turn ensures protection to licensed users operating on the same frequency as the WSDs.

Table 1. FSPL RMSE values (dB) for each location

Path Loss	RMSE (dB)		
Free Space Path Loss	Location1	Location 2	Location 3
	14.22	20.72	18.73

Table 2. ITU R.P. 1411 – 11 Section 4.1.2 RMSE values (dB) for each location

Path Loss	RMSE (dB)		
	Location 1	Location 2	Location 3
Section 4.1.2 LoS	10.26	15.81	8.30
Section 4.1.2 LoS	13.70	6.39	19.61

5.2. Recommendation ITU-R P.1411 – 11 Section 4.1.2 Line-of-Sights (LoS) Path

In calculating and graphing the plots of LoS lower bound (LoS_L) and LoS upper bound (LoS_U), the following parameters were used: AP height Htx = 1.7 m, STA height Hrx = 1.2 m, and operating frequency f = 593 MHz Following Equation 6, the breakpoint distance R_{bp} is computed as 16.13 m. At this breakpoint, the value of the basic transmission loss L_{bp} using Equation 8 is computed to be 45.89 dB. Subject to the distance d between AP and STA, the approximate lower bound (LoS_L) and the estimated upper bound (LoS_U) were computed using Equations 5 and 7, respectively. Note that 20 dB is the fade margin of the upper bound.

For Location 1 (Figure 6(a)), about 90% of the measured path losses lie above the LoS_L fitted line with an RMSE value of 10.26 dB (Table 5), mostly due to underestimation, but this should be read alongside the LoS_U fitted line that puts all data points below it with an overestimation RMSE value of 13.70 dB (Table 5). Taken together, the LoS_U upper bound can provide sufficient interference protection to existing licensed users. However, it can also result in needlessly restricting the regions where the WSDs can operate. In contrast, the LoS_L lower bound has overestimated path loss in the 80 to 100 – meter location from the AP. This translates to particular areas where primary users may not be adequately protected from interference from WSDs.

The approximate lower bound LoS_L in Figure 6(b) underestimated path losses by 15.81 dB, which is considerably high and has the effect of failure to provide interference protection to licensed users. On the other hand, the approximate upper bound LoS_U overestimated by 6.39 dB, which is a relatively moderate value to limit areas where IEEE 802.11af-based WSDs can operate. Both RMSE values for Location 2 are listed in Table 5. Notice, however, that beyond 90 meters, both LoS_L and LoS_U correctly provide the appropriate lower and upper bounds for measured path losses.

Based on Table 2 and Figure 6(c), Location 3 has the lowest approximate lower bound LoS_L RMSE value of 8.30 dB due mainly to underestimation and the highest approximate upper bound LoS_U RMSE value of 19.61 dB this time, due to overestimation - the highest among the recorded LoS_U RMSE values. The overestimation is worse at 205 – meters onward, averaging 25 dB prediction error, resulting in a very limited area where WSDs can operate, hence negating the intent of allowing spectrum sharing among primary and secondary users.

Section 4.1.2 of the ITU Recommendation approximates LoS_L and LoS_U values in the context of WLAN in TV white space. It is supposed to give guidance for path loss estimation models that are accurate. The LoS_L is assumed to give an optimum RMSE value that will underestimate path loss sufficient to protect primary users from damaging interference induced by WSDs. On the other hand, the LoS_U should provide an optimum RMSE value that will overestimate path loss without imposing too many limitations on the areas where WSDs can operate. Based on the fitted data for each test site and as listed in Table 4, the optimal values for LoS_L are 6.36 dB (Location 1) and for LoS_U 8.36 dB.

5.3. ITU-R P.1411 - 11 Recommendation Section 4.3.1

Recommendation Section 4.3.1, also known as the site-general model, provides statistics on location variability within the Line-of-Sight (LoS) region. This model considers parameters such as the operating frequency f=593 MHz and the distance d in meters, which can vary depending on the experimental site. For instance, at Location 1, distances range from 5 meters to 165 meters; at Location 2, the distance is 155 meters; and at Location 3, it is 210 meters.

Location variability explains the changes in long-term statistics observed from one path to another, influenced by factors like differences in terrain profiles or environmental variations along the routes. Typically expressed as a percentage from 1% to 99%, this indicates the portion of locations where the median field strength is projected to be less than or equal to the actual received field strength. Using Equation 10, ΔLos (p), which represents the Line-of-Sight location correction for a given location percentage (%), is computed with a standard deviation δ=7 dB, resulting in values of 10.6 dB for (90%) and 20.3 dB for (99%). Given p and d, Equation 9 is then utilized to calculate the path attenuation $LoS(d,p)$.

Table 3. ITU R.P. 1411 - 11 Section 4.3.1 RMSE Values (dB) for Each Site

Path Loss	RMSE (dB)		
	Location 1	Location 2	Location 3
Section 4.3.1 p (90%)	6.19	11.05	10.18
Section 4.3.2 p (99%)	9.23	6.15	7.13

Figure 7 shows the measured path loss distribution fitted with the curves of basic transmission path loss for 90% and 99% locations variability predicted by the model in the LoS region. The dots represent measured data, and the purple and light blue lines show the results obtained by applying Section 4.3.1 location percentages of 90% and 99%, respectively.

For Location 1 (Figure 7(a)), the distribution of data points around the p(90%) model shows an underestimation of most data points, particularly noticeable beginning at 100 meters, while overestimation is obvious in the range of 65 to 95 meters for a 6.19 dB RMSE value. For the p(99%) location percentage, about 81% of the measured path losses were overestimated in 81% of the locations where the measurements were taken. The overestimation is from 2.3 dB to 16 dB, resulting in an RSME of 9.23 dB.

Referring to Figure 7(b) for Location 2, the use of p(90%) location variability predicted an underestimation of path loss from more than 10 meters onward, ranging from 3 dB to 19 dB, while overestimation ranges from 1 to 4 dB at distances lower than 10 meters. This results in an RSME of about 11.05 dB due, in general, to underestimation.

In the same figure, the use of p(99%) location variability provides a 64% underestimation of the measured path loss over the given span from 0.4 dB as the lowest to 9.6 dB as the highest. On the other hand, the same location variability provides a 36% overestimation ranging from 3 to 14 dB. RSME for this model is an overestimation of 6.15 dB.

For the entire range of Location 3 (Figure 7(c)), all measured path losses for the p(90%) location variability model were underestimated by 0.1 dB to 11 dB for an underestimation RSME value of 10.18 dB. The p(99%) location percentage model has the observed path losses fluctuating in the fitted model. It overestimated from 1 to 65 meters distance, underestimated from 70 to 180 meters and then overestimated again beginning at 185 meters. The RMSE value of 7.13 dB for this location percentage is mostly due to underestimation. Table 3 summarizes the results mentioned above.

5.4. Linear and Logarithmic Regression Models

The use of the Linear Regression model is always preceded by an indication of some degree of linearity between the independent variable (x, distance in meters) and the dependent variable (y, path loss in dB) in its scattered plots, as Figure 8 illustrates. Using Equations 15 and 16, the values of the sample intercept b_0 and the sample slope b_1 were obtained for each site or location, respectively. These values were then used to generate the regression model in Equation 14. Table 4 summarizes the linear and logarithmic regression models and the corresponding values of their respective RMSE (dB) and R-squared (R^2) for each site.

Based on the linear regression model for Location 1, for every 5-meter increase in the distance x_i, the path loss is expected to increase by 0.2615 dB. If the separation distance between the AP and STA is theoretically zero, the expected/predicted path loss is 54.237 dB. What the R^2 value of about 84% suggests that 84% of the SST can be explained by utilizing the estimated regression model to predict path loss. The 16 %remainder is due to the error in the model itself.

For Location 2, for the same increment in distance x_i, the path loss is expected to increase by 0.2947 dB, and the expected path loss is 59.921 dB when the distance is zero. A 72.28% of the SST can be expounded by using the estimated regression model to predict path loss. The remainder is due to the error. And for Location 3, for every 5-meter increase in the distance x_i, the path loss is expected to increase by 0.0988 dB. If the distance is zero, the predicted path loss is 71.325 dB. For Location 3, the generated regression model can only explain only about 38% of the total sum of squares while a high 62% is due to the error in the regression model to estimate path loss itself. In general, for the same 5 – m increment in distance for all sites, the increase in estimated path loss is lowest at 0.1 dB in Location 3, while the increase in both Locations 1 and 2 is almost identical at 0.3 dB. However, the inherent path loss, that is $x_i = 0$, or the separation distance between the AP and STA is theoretically zero, is largest at Location 3 with 71 dB, followed by Location 2 with 59 dB and Location 1 with 54 dB. In terms of goodness - of – fit criterion, the R^2 values obtained for Location 1 (87%) and Location 2 (72%) can be considered a good fit, while an R^2 value of 38% for Location 3 is considered a bad fit.

Examining the distribution of data points representing measured path losses in all experimental sites in Figure 8 clearly characterizes a logarithmic function that increases swiftly at first but then gradually slows as the distance increases. Hence, it is possible to fit a linear model with a log-transformed independent variable to come up with an Equation 17. Equation 17 should be interpreted as a 1% increase in the independent variable x_i increases the dependent variable $\hat{y}_i$ by $(b_1/100)$ units. In essence, a proportional change in the independent variable leads to a consistent change in the dependent variable. Based on the said equation, the derived logarithmic regression models for each site are tabulated in Table 4, including also its corresponding RMSE and R^2 values.

The logarithmic regression model for Location 1 means that a 1% increase in the distance x_i would increase the estimated path loss $\hat{y}_i$ by $\frac{10.315}{100}$ or 0.10 dB. For Location 2, since b_1 is 12.375, then the estimated path loss is expected to increase by 0.12 dB and finally, an increase of 0.09 or roughly 0.10 dB for predicted path loss for the location 3 whose b_1 is equal to 9.611 is expected. It is safe to say that for all sites, roughly a 0.1 dB loss is expected.

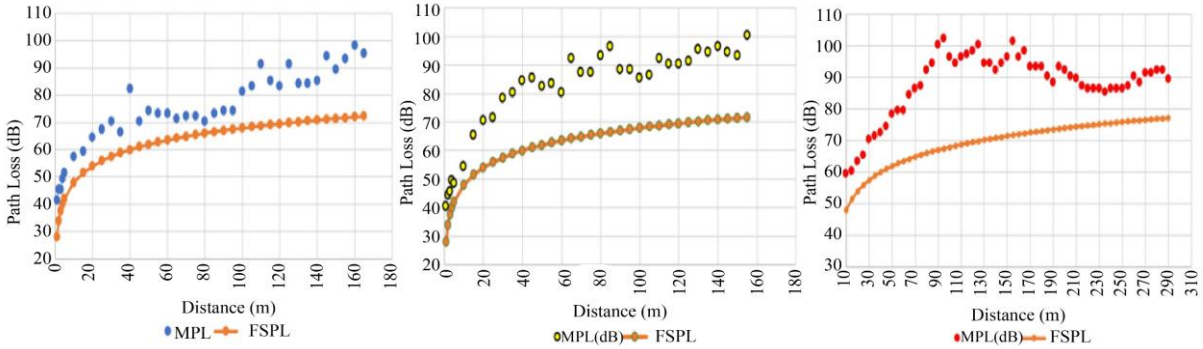

(a) (b) (c)

Fig. 5 Graph of Measured Path Loss (MPL) with free space path loss: (a) Location 1, (b) Location 2, and (c) Location 3.

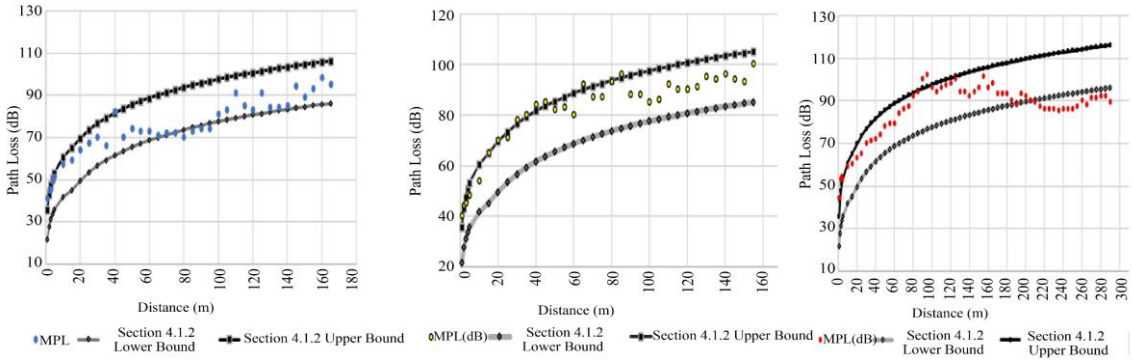

(a) (b) (c)

Fig. 6 Graph of Measured Path Loss (MPL) with ITU-R P. 1411-11 Sec. 4.1.2 loss lower and upper bounds: (a) Location 1, (b) Location, 2 and (c) Location 3.

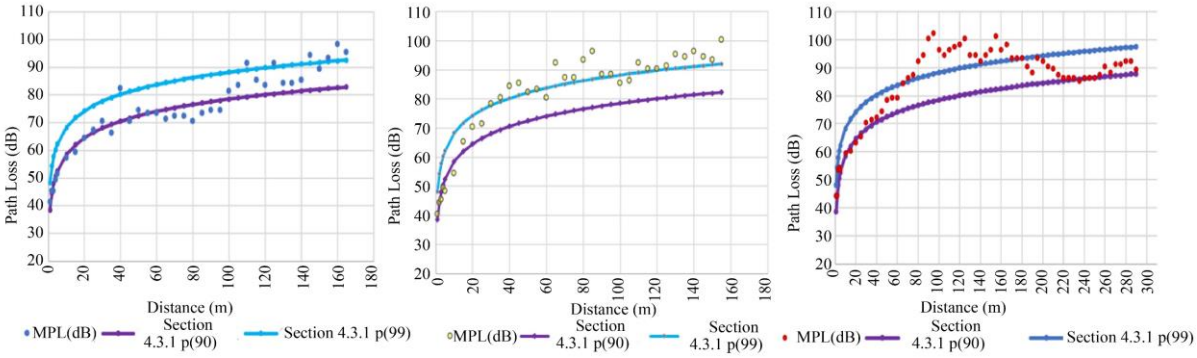

(a) (b) (c)

Fig. 7 Graph of Measured Path Loss (MPL) with ITU-R P. 1411-11 Sec. 4.3.1 p(90%) and p(99%): (a) Location 1, (b) Location 2 and (c) Location 3.

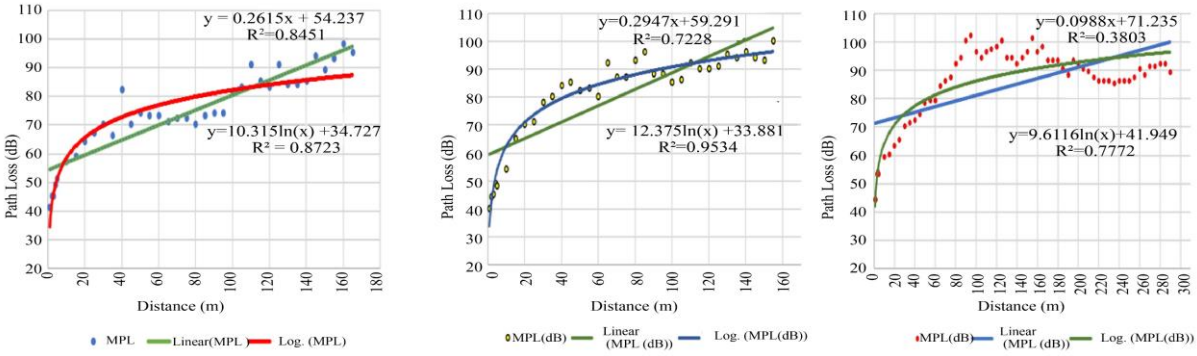

(a) (b) (c)

Fig. 8 Graph of Measured Path Loss (MPL) with linear and logarithmic regression models: (a) Location 1, (b) Location 2, and (c) Location 3.

Table 4. Regression model equations, RMSE (dB) and R^2 values for each location

Path Loss	RMSE (dB)		
	Location 1	Location 2	Location 3
Linear Regression	$\hat{y}_i = 54.237 + 0.2615x_i$ RMSE-> 5.8 (R^2=0.8451)	$\hat{y}_i = 59.291 + 0.2947x_i$ 8.93 (R^2=0.7228)	$\hat{y}_i = 71.235 + 0.0988x_i$ 8.41 (R^2=0.3803)
Logarithmic Regression	$\hat{y}_i = 34.727 + 10.315\ln(x_i)$ RMSE-> 5.26 (R^2=0.8723)	$\hat{y}_i = 33.881 + 12.375\ln(x_i)$ 3.65 (R^2=0.9534)	$\hat{y}_i = 41.949 + 9.6116\ln(x_i)$ 6.33 (R^2=0.7772)

If the separation distance between the AP and STA is theoretically zero, the inherent attenuation for Locations 1, 2 and 3 are 35, 34 and 42 dB, respectively. As can be deduced from the results, just like in the linear regression models, Location 3 still provides the largest inherent path loss at 42 dB. Looking at the R^2 values or Coefficient of Determination listed in Table 4 for Logarithmic regression models, all of them provide a relatively good fit, with Location 2 indicating the best fit with R^2 value of 95%, which means that only 5% can be attributed to the error in the model itself. For Location 1, the estimated regression model can explain about 87% of the total sum of squares to estimate path loss. The remainder of 13 % is due to the error. For Location 3, about 22% is due to the error in the regression model to predict path loss itself, while 78% of the variability can be explained by using the generated regression equation.

6. Conclusion

This study conducts experimental field tests in three different RF environments inside a suburban University campus to determine the appropriate model for path loss for an IEEE 802.11af–based wireless LAN. Measurements were taken and then fitted to the FSPL model, to the appropriate sections of ITU-R P.1411 – 11, and the linear and logarithmic regression models to determine the prediction model that best fits the path loss. As Table 5 shows, the best RMSE value is given by logarithmic regression models that gave a mean estimation error of 5 dB for all test locations studied and whose values of R^2 or Coefficient of Determination provides a relatively good fit, with Location 2 indicating the best fit with R^2 value of 95%, which means that only 5% can be attributed to the error in the model itself. However, while lower values of the RMSE indicate better fit, these values should also be interpreted in the context of an IEEE 802.11af–based network that operates on a spectrum sharing principle; hence, interference to primary users must be avoided. An overestimating path loss model can lead to limiting the coverage areas where white space devices can operate and an underestimating model will lead to failure in protecting primary users from destructive interference emitted by IEEE 802.11af devices. In this framework, the study also concludes that the FSPL model can accurately provide a lower bound path loss for all sites with an average overestimation of 18 dB, ensuring adequate protection to primary users from unwanted interference that may come from IEEE 802.11af devices. Further, based on the fitted data for each test site and as can be verified from Table 5, the use of Section 4.1.2 approximate lower (LoS_L) and upper (LoS_U) bounds as well as Section 4.3.1 of ITU – R.P. 1411 -11 as prediction models for path loss are invariably site - dependent.

Funding Statement

The research described in this paper received funding from the National Institute of Information and Communications Technology, Japan, under the project focused on "TV White Space (TVWS) Experimental for Application in Remote Area." Additionally, the researchers express gratitude to DOST - Philippines for their support.

Acknowledgments

The authors extend their gratitude to the Administration of the University of San Carlos for granting permission to carry out field tests and measurements on the University campus. They also appreciate the assistance provided by the students of the Department of Electrical and Electronics Engineering.

Table 5. Summary of RMSE values (dB) for each site for each path loss model

Experimental Locations	Path Loss Model RMSE (dB)						
	FSPL	Section 4.1.2 LoS Lower	Section 4.1.2 LoS Upper	Section 4.3.1 p(90%)	Section 4.3.1 p(99%)	Linear Regression	Logarithmic Regression
Location 1	14.22	10.26	13.70	6.19	9.23	5.8 (R^2=0.8451)	5.26 (R^2=0.8723)
Location 2	20.72	15.81	6.39	11.05	6.15	8.93 (R^2=0.7228)	3.65 (R^2=0.9534)
Location 3	18.73	8.30	19.61	10.18	7.13	8.41 (R^2=0.3803)	6.33 (R^2=0.7772)

References

[1] Dynamic Spectrum Alliance: Worldwide Commercial Deployments, Pilots, & Trials, pp. 1-23, 2015. [Online]. Available: https://dynamicspectrumalliance.org/wp-content/uploads/2015/07/Pilots-and-Trials-Brochure_July-15.pdf

[2] "IEEE Standard for Information Technology - Telecommunications and Information Exchange between Systems - Local and Metropolitan Area Networks - Specific Requirement - Part 11: Wireless LAN Medium Access Control (MAC) and Physical Layer (PHY) Specifications Amendment 5: Television White Spaces (TVWS) Operation," *IEEE Std 802.11*, 2014. [Google Scholar]

[3] Kentaro Ishizu et al., "Field Experiment of Long-Distance Broadband Communications in TV White Space Using IEEE 802.22 and IEEE 802.11af," *2014 International Symposium on Wireless Personal Multimedia Communications*, Sydney, NSW, Australia, pp. 468-473, 2014. [CrossRef] [Google Scholar] [Publisher Link]

[4] Antonio Montejo et al., "Implementation of a Multi-Hop Network at the University Campus Using an IEEE 802.11af-Compliant Network," *2017 20th International Symposium on Wireless Personal Multimedia Communications*, Bali, Indonesia, pp. 173-180, 2018. [CrossRef] [Google Scholar] [Publisher Link]

[5] Jeric G. Brioso et al., "Vehicle to Vehicle Communications at Suburban Environment Using IEEE 802.11af Compliant Devices," *2018 21st International Symposium on Wireless Personal Multimedia Communications*, Chiang Rai, Thailand, pp. 85-89, 2018. [CrossRef] [Google Scholar] [Publisher Link]

[6] Jeric G. Brioso et al., "Evaluation of IEEE 802.11af Compliant Devices for Vehicle to Infrastructure Communications in Suburban Environment," *2018 IEEE Vehicular Networking Conference*, Taipei, Taiwan, pp. 1-4, 2018. [CrossRef] [Google Scholar] [Publisher Link]

[7] Tsuyoshi Shimomura, Teppei Oyama, and Hiroyuki Seki, "Analysis of TV White Space Availability in Japan," *2012 IEEE Vehicular Technology Conference*, Quebec City, QC, Canada, pp. 1-5, 2012. [CrossRef] [Google Scholar] [Publisher Link]

[8] Theodore S. Rappaport, *Wireless Communications: Principles and Practice*, Prentice Hall PTR, pp. 1-707, 2002. [Google Scholar] [Publisher Link]

[9] Hirokazu Sawada et al., "Path Loss and Throughput Estimation Models for an IEEE 802.11af Prototype," *2015 IEEE 81st Vehicular Technology Conference*, Glasgow, UK, pp. 1-5, 2015. [CrossRef] [Google Scholar] [Publisher Link]

[10] Yee-Loo Foo, "Keep-Out Distance of the IEEE 802.11af System from Digital TV Broadcast Contour," *TENCON 2017 - 2017 IEEE Region 10 Conference*, Penang, Malaysia, pp. 1185-1188, 2017. [CrossRef] [Google Scholar] [Publisher Link]

[11] International Telecommunications Union, Radio Communications Bureau, "*Recommendation ITUR P.1411-11: Propagation Data and Prediction Methods for the Planning of Short-Range Outdoor Radio Communication Systems and Radio Local Area Networks in the Frequency Range 300MHz to 100 GHz*," P Series, ITU Recommmendations, pp. 1-52, 2021. [Google Scholar] [Publisher Link]

[12] P. Almorox-Gonzalez, and J.I. Alonso, "Software Tool for Planning Wireless Local Area Networks (WLAN)," *The European Conference on Wireless Technology*, Paris, France, pp. 387-390, 2005. [CrossRef] [Google Scholar] [Publisher Link]

[13] Mingming Li, and Dongxu Wang, "Indoor Coverage Performance Comparison between IEEE 802.11g and IEEE 802.11 ah of Wireless Nodes in M2M Network," *Internet of Vehicles-Technologies and Services: First International Conference*, Beijing, China, pp. 211-217, 2014. [CrossRef] [Google Scholar] [Publisher Link]

[14] Siva Priya Thiagarajah et al., "An Investigation on the Use of ITU-R P.1411-7 in 802.11N Path Loss Modelling," *Progress In Electromagnetics Research Letters*, vol. 50, pp. 91-98, 2014. [CrossRef] [Google Scholar] [Publisher Link]

[15] Siva Priya Thiagarajah et al., "Applying ITU-R P.1411-7 Estimation for Urban 802.11N in Network Planning," *Progress In Electromagnetics Research Letters*, vol. 54, pp. 55-59, 2015. [CrossRef] [Google Scholar] [Publisher Link]

[16] Supachai Phaiboon, and Pisit Phokharatkul, "Multi-Boundary Empirical Path Loss Model for 433 MHz WSN in Agriculture Areas Using Fuzzy Linear Regression," *Sensors*, vol. 23, no. 7, pp. 1-20, 2023. [CrossRef] [Google Scholar] [Publisher Link]

[17] Yan Zhang et al., "Path Loss Prediction Based on Machine Learning: Principle, Method, and Data Expansion," *Applied Sciences*, vol. 9, no. 9, pp. 1-18, 2019. [CrossRef] [Google Scholar] [Publisher Link]

[18] Usman Sammani Sani, Owais Ahmed Malik, and Daphne Teck Ching Lai, "Improving Path Loss Prediction Using Environmental Feature Extraction from Satellite Images: Hand-Crafted vs. Convolutional Neural Network," *Applied Sciences*, vol. 12, no. 15, pp. 1-24, 2022. [CrossRef] [Google Scholar] [Publisher Link]

[19] Moamen Alnatoor, Mohammed Omari, and Mohammed Kaddi, "Path Loss Models for Cellular Mobile Networks Using Artificial Intelligence Technologies in Different Environments," *Applied Sciences*, vol. 12, no. 24, pp. 1-23, 2022. [CrossRef] [Google Scholar] [Publisher Link]

[20] Konstantinos Gatsis, "Linear Regression over Networks with Communication Guarantees," *Proceedings of the 3rd Conference on Learning for Dynamics and Control*, vol. 144, pp. 767-778, 2021. [Google Scholar] [Publisher Link]

[21] Yongjun Zhang, and Ling Ye, "Indoor Localization Method Based on AP and Local Linear Regression Algorithm," *2017 IEEE 17th International Conference on Communication Technology*, Chengdu, China, pp. 1122-1126, 2017. [CrossRef] [Google Scholar] [Publisher Link]

[22] Liangping Ma et al., "Understanding Linear Regression for Wireless Sensor Network Time Synchronization," pp. 325-328, 2007. [Google Scholar]

[23] Manish Kumar Sahu, and Sunil Patil, "Linear Regression Based Power Optimization of Wireless Sensor Network in Smart City," *IOP Conference Series: Materials Science and Engineering*, vol. 1085, no. 1, pp. 1-8, 2021. [CrossRef] [Google Scholar] [Publisher Link]

[24] "IEEE Standard for Information Technology - Telecommunications and Information Exchange between Systems - Local and Metropolitan Area Networks - Part 11: Wireless LAN Medium Access Control (MAC) and Physical Layer (PHY) Specifications," *IEEE Computer Society*, pp. 1-198, 2014. [Google Scholar]

[25] Robert Kissell, and James Poserina, *Optimal Sports Math, Statistics and Fantasy*, Elsevier Science, pp. 1-352, 2017. [Google Scholar] [Publisher Link]

[26] David Freedman, *Statistical Models: Theory and Practice*, Cambridge University Press, pp. 1-442, 2009. [Google Scholar] [Publisher Link]

[27] John Fox, and Sanford Weisberg, *An R Companion to Applied Regression*, SAGE Publications, pp. 1-608, 2018. [Google Scholar] [Publisher Link]